

# Distribution and Mobility of Zn, Pb and Cd in a Sewage Sludge-Amended Soil

Dominique Proust, Vivien Mathé, François Lévêque

LIENSs UMR 7266 CNRS-Université de La Rochelle, La Rochelle, France.  
Email: dominique.proust@univ-lr.fr

Received October 21<sup>st</sup>, 2013; revised November 21<sup>st</sup>, 2013; accepted November 28<sup>th</sup>, 2013

Copyright © 2013 Dominique Proust *et al.* This is an open access article distributed under the Creative Commons Attribution License, which permits unrestricted use, distribution, and reproduction in any medium, provided the original work is properly cited.

## ABSTRACT

The distribution of the metallic trace elements (MTE) Zn, Pb and Cd in a sludge-amended soil and their partitioning in specific soil microsystems are studied by comparing their contents in amended and control soils. This comparison is achieved at the metric scale of the bulk soil horizons and at the micrometric scale of the weathering microsites (weathering rock-forming minerals and their specific weathered products). The chemical analyses of the MTE in the bulk samples do not show any anthropic contamination of the amended soil with repeated sewage sludge spreading. The chemical analyses of the bulk < 2  $\mu\text{m}$  clay fractions indicate the occurrence of local MTE concentrations and vertical migration in deeper soil horizons. Precise chemical analyses in the weathering microsites indicate that, as a general rule and whatever microsite is considered, Zn, Pb, and Cd accumulate in clay minerals from surface horizons where the sludge was spread. On the contrary, the vertical MTE migration is restricted to the connected macroporosity of the fissural system filled with clay minerals and does not affect the weathering clays of rock-forming minerals. Such MTE mobility through the fissural system gives rise to two main environmental problems: 1) Zn, Pb, and Cd have the potential to move several meters deep along fissures in the soil profiles and may represent potential contaminants for unconfined aquifer and 2) because plant root system grows preferentially along soil fissural pattern, it may adsorb migrating MTE.

**Keywords:** Soil; Metallic Trace Elements; Heavy Metals; Clay Minerals

## 1. Introduction

As a result of the substantial increase in waste water treatment plants in Europe over the past thirty years, problems have emerged in disposing of sewage sludges in an environmentally sound manner. Sludges landfilling, incinerating or landspreading are the most currently used practices. Properly constructed and monitored landfills are very expensive and will be forbidden in Europe in 2015 because they may generate point-source contaminations due to waste concentrations. Sludge incinerating is also expensive due to the need for sludge dehydration prior to burning and the cost of incinerators preventing air pollution. These practices have thus decreased in the last decade in favor of sludge spreading on cropland, especially in France [1]. This spreading method is considered both a low cost disposal method as well as a source of nutrient-rich fertilizer. However, the use of sewage sludge as a fertilizer in soil remains a debated subject. As a source of plant nutrients (especially P and

N) and organic matter, sewage sludge is a beneficial soil amendment. Nevertheless, these sludges originate from industrial and urban by-products treatments and may contain MTE that can be toxic at very low concentration: for instance, Cd concentration cannot exceed  $2 \text{ mg}\cdot\text{kg}^{-1}$  in non polluted soils [2-4].

The MTE in soils result in 1) the natural geochemical stock produced by the weathering of the parent rock [5-7], and 2) the anthropogenic contamination by repeated sludge spreading [8,9] and/or atmospheric deposition [10,11]. In such a pedological context, the chemical reactions of weathering will control the solubility, mobility and, as a consequence, the concentration of MTE in soils. The weathering reactions result in 1) the release of the MTE from the dissolving primary minerals and 2) their sorption onto clay minerals, hydrous oxides, and organic matter. The pH, together with the redox potential is also active parameter on the mobility of MTE in soils: a decrease in soil pH and in redox potential increases MTE

release from soil [12-14].

Several mineralogical studies showed that the chemical reactions of weathering and their associated metal release were operating in specific soil microsystems with their own solid and solution chemical properties [15-17]. Such microsystems are typically composite aggregates of weathering rock-forming minerals, newly-formed clay minerals, oxi-hydroxides, and organic matter moistened with soil solutions. Even though MTE bulk concentrations could be indicators of global soil contamination, they result from the partial MTE concentrations in each of these microsystems. In that meaning, the detailed analysis of contaminated soils with MTE requires to know the bulk metals content in the soil but also their partial contents in the soil microsystems in which they are retained.

The present study was undertaken to estimate the impact of long-term sludge application upon Zn, Pb, and Cd distribution and migration in soil. In the bulk soil study, MTE concentrations are compared in control and amended soils to characterize the extent to which spreaded metals may have moved throughout the soil profile. In the micrometric study, MTE are analysed in the weathering microsystems to detect possible zones of metals accumulation within soil and weathered parent rock.

## 2. Materials and Methods

### 2.1. Soils and Sampling Process

The soils were sampled in a dioritic massif 25 km in the South of Limoges, Haute-Vienne (**Figure 1(a)**). They are inceptisols covering a hill 305 meters high at Labrousse locality. The two soils were sampled on the same dioritic parent-rock (**Figures 1(b)** and **(c)**): 1) the Amended Soil profile (AS) that received for ten years wet sewage sludges heavily loaded with Zn, Pb, and Cd, and 2) the Control Soil (CS) that is free of sludge spreading.

The two soils are moderately drained, deep (1.00 to 1.50 m to C horizon) inceptisols with the typical A, Bw, and C horizons sequence. The R horizon, *i.e.* unweathered parent rock (**Figure 1(d)**), is a diorite which appears as a “salt and pepper” coarse-grained rock made up of major amphiboles, feldspars, and minor quartz.

Each soil sample was carefully collected as undisturbed block using plastic core samplers (20 cm length) with cutting edges, smoothly and continuously pushed into the soil to preserve the original fabric of the soil and to prevent the sample metal contamination. Each sample was further divided into two subsamples. The first was devoted to the bulk chemical analysis and the X-ray diffraction (XRD) study whereas the second part was used for thin sections preparation.

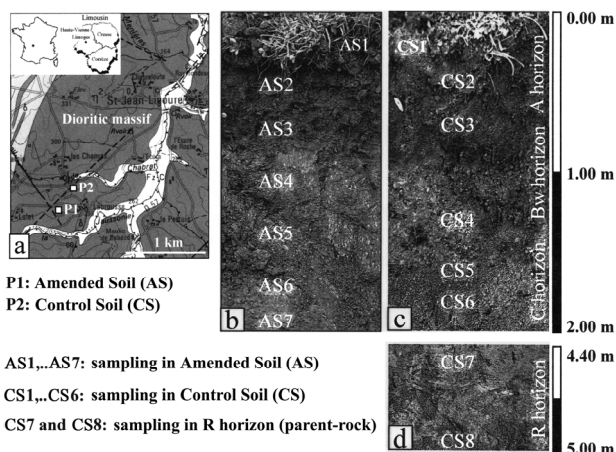


**Figure 1. Location and sketch of the soil profiles. (a) Geological setting; (b) Amended soil (AS); (c) Control soil (CS); (d) R horizon (parent-rock).**

### 2.2. Bulk Chemical and X-Ray Diffraction Analyses

An aliquot quantity of the first subsample (5 g) was crushed into agate mortar down to less than 50  $\mu\text{m}$  size and 300 mg of total powder (fused with  $\text{LiBO}_2$  and dissolved in 1N  $\text{HNO}_3$ ) was used for the bulk chemical analysis of major and trace elements with ICP-AES and ICP-MS (PERKIN ELMER 5000 spectrometer) by the Service d'Analyse des Roches et des Minéraux, (SARM), CRPG-CNRS (Vendoeuvre-lès-Nancy, France). The major and trace element concentrations were expressed in wt.% and  $\text{mg}\cdot\text{kg}^{-1}$ , respectively. In order to calculate geochemical mass balances from the bulk chemical analyses, the apparent density of each sample was obtained using the hydrostatic balance.

The rock-forming minerals and their weathering products were identified using XRD on random powders with a PHILIPS PW 1730 diffractometer (40 kV, 40 mA), Fe-filtered  $\text{Co}\alpha$  radiation and a stepping motor-driven with a DACO-MP recorder and the Diffrac-AT software (Socabim). The clay minerals were extracted from the soil samples by ultrasonic treatment and centrifugation of the supernatant in order to separate the less than 2  $\mu\text{m}$  fraction. These clay minerals were then identified by XRD on random powders, Ca-oriented and Ca-glycolated oriented preparations.

### 2.3. Electron Probe Micro Analyses

The second subsample was devoted to the Electron Probe Micro Analyses (EPMA). Thin sections were prepared following the method of Camuti and McGuire [18]: after hardening using vacuum impregnation unit (BROT 1.04.05, 100 mbars) with ARALDITE 2020 epoxy resin and 20% acetone thinner, samples were cut and thin sections obtained through polishing with silicon carbide

(17 and 9  $\mu\text{m}$  particle sizes) and diamond calibrated powders (6, 3, 1 and 0.25  $\mu\text{m}$  particle sizes).

Representative pedofeatures as well as weathering microsites were first located on the thin sections, marked with black circle under an optical microscope and then “*in situ*” analysed for major and trace elements. EPMA were obtained using a CAMECA SX 50 electron microprobe (Service CAMPARIS, Université Paris VI) equipped with wavelength-dispersive spectrometers (WDS). The microprobe was calibrated using synthetic and natural oxides. Corrections were made with a ZAF program. A specific trace program with the electron microprobe was developed [19] to analyse MTE in small volumes with detection limits closed to 6 - 8  $\text{mg}\cdot\text{kg}^{-1}$ . Major elements analyzes were performed at 15 kV and 4 nA prior to trace element analysis performed at higher voltage (30 kV) and higher beam current (100 nA and 500 nA for small and large minerals, respectively) in order to improve detection limits. The spot sizes varied from 1 to 5 - 10  $\mu\text{m}$  to limit beam damage. The counting time was 10 s per major element and 1000 s per trace element. Major and trace elements are expressed respectively in wt% and  $\text{mg}\cdot\text{kg}^{-1}$ .

### 3. Results

#### 3.1. Parent Rock Mineralogy

The parent rock mineralogy was studied from the CS8

sample of the “R” horizon (**Figure 1(d)**). This sample is the unaltered fresh rock with the highest apparent density and low loss on ignition (L.O.I., **Table 1**). The modal composition obtained from 3000 points counting gives a typical dioritic mineralogical composition with amphiboles (38%), plagioclases (32%), orthoclase (12%) with minor quartz (8%), albite (7%), and titanomagnetite (3%). The EPMA of the major elements in the rock-forming minerals (**Table 2**) shows that the amphiboles are calcic hornblende whereas plagioclases are andesine with 48 % anorthite content. The EPMA of the MTE (**Table 2**) shows that amphiboles are the major MTE-bearing minerals with high Zn and Pb concentrations (180  $\text{mg}\cdot\text{kg}^{-1}$  for Zn and 73  $\text{mg}\cdot\text{kg}^{-1}$  for Pb) and very low Cd concentrations (6  $\text{mg}\cdot\text{kg}^{-1}$ ). The feldspars show significantly lower MTE contents with almost similar concentrations in orthoclase, albite and plagioclase (14 - 20  $\text{mg}\cdot\text{kg}^{-1}$  for Zn, 19 - 27  $\text{mg}\cdot\text{kg}^{-1}$  for Pb, and 2 - 4  $\text{mg}\cdot\text{kg}^{-1}$  for Cd).

#### 3.2. Weathering Mass Balances

Many mass balance models have been published in the literature to investigate and quantify the chemical change in rock during its interaction with altering fluids [20-23].

Most of these models are based upon the general equation of Gresens [20] where bulk densities and chemical data of altered rocks are compared to a reference rock in order to quantify the losses or gains of elements resulting

**Table 1** Bulk chemical analyses of major elements (wt.%) and heavy metals (Zn, Pb, Cd,  $\text{mg}\cdot\text{kg}^{-1}$ ), and apparent density ( $\text{d}$ ,  $\text{g}\cdot\text{cm}^{-3}$ ) of control soil (CS) and amended soil (AS) samples.

Depth	CS8	CS7	CS6	CS5	CS4	CS3	CS2	CS1	AS7	AS6	AS5	AS4	AS3	AS2	AS1
(m)	4.85	4.50	1.80	1.60	1.30	0.65	0.40	0.20	1.90	1.70	1.40	1.10	0.70	0.40	0.20
SiO <sub>2</sub>	48.79	47.24	47.99	46.69	46.03	46.76	50.12	46.07	50.90	50.21	51.27	52.34	50.83	51.23	50.95
TiO <sub>2</sub>	1.08	1.27	1.14	1.29	1.27	1.23	1.29	1.37	1.28	1.24	1.27	1.31	1.42	1.48	1.51
Al <sub>2</sub> O <sub>3</sub>	18.78	18.25	19.10	18.95	18.32	18.78	21.60	18.98	18.56	18.47	18.41	17.93	18.67	17.53	18.74
Fe <sub>2</sub> O <sub>3</sub> <sup>a</sup>	9.58	11.04	10.03	10.88	11.68	10.97	7.42	9.75	8.07	8.53	7.99	7.97	8.06	8.55	8.00
MnO	0.17	0.20	0.18	0.19	0.20	0.19	0.11	0.16	0.14	0.15	0.15	0.12	0.11	0.12	0.11
MgO	4.47	4.86	4.20	4.60	4.96	4.76	2.47	4.09	3.25	3.44	3.19	3.29	3.36	3.36	3.08
CaO	7.52	8.06	6.97	7.50	7.91	8.01	4.38	6.26	5.70	5.83	5.24	2.11	3.55	2.41	4.26
Na <sub>2</sub> O	3.54	3.17	3.36	3.06	2.80	3.08	4.10	2.82	3.19	3.08	3.19	3.50	2.96	3.18	3.25
K <sub>2</sub> O	1.44	1.35	1.50	1.16	1.31	1.20	1.59	1.67	2.54	2.35	2.69	3.70	2.86	3.14	2.63
P <sub>2</sub> O <sub>5</sub>	0.59	0.67	0.60	0.65	0.67	0.63	0.50	0.57	0.00	0.00	0.00	0.00	0.00	0.00	0.00
LOI <sup>b</sup>	3.77	3.46	4.68	5.10	4.80	4.37	6.86	8.53	5.91	6.48	6.19	7.77	7.74	8.49	6.72
Total	99.73	99.57	99.75	100.06	99.95	99.96	100.43	100.26	99.53	99.79	99.59	100.04	99.56	99.49	99.24
Zn	111.18	124.46	113.06	119.32	126.08	120.42	88.24	115.56	90.11	93.04	90.64	82.00	94.64	95.27	99.29
Pb	16.46	22.46	15.56	18.68	14.84	20.18	18.28	38.24	20.08	17.00	19.09	16.24	21.00	29.00	39.08
Cd	<d. l.	<d. l.	<d. l.	<d. l.	<d. l.	<d. l.	<d. l.	<d. l.	0.13	0.20	0.26	0.25	0.32	0.30	0.33
d	2.92	2.55	2.65	2.49	2.39	2.43	2.13	2.07	2.56	2.37	2.34	2.25	2.14	2.09	2.05

<sup>a</sup>Total iron expressed as Fe<sub>2</sub>O<sub>3</sub>; <sup>b</sup>Loss on ignition, < d. l.: lower than detection limit.

**Table 2. EPMA of major elements (wt.%), MTE (mg·kg<sup>-1</sup>) and structural formulae of rock-forming minerals from control soil CS8 sample.**

	Amphibole	Orthoclase	Albite	Plagioclase
	Mean	Mean	Mean	Mean
SiO <sub>2</sub> <sup>a</sup>	42.54 (0.88)	61.91 (2.19)	67.87 (0.92)	58.24 (1.25)
TiO <sub>2</sub>	1.31 (0.36)	0.04 (0.05)	0.05 (0.06)	0.06 (0.19)
Al <sub>2</sub> O <sub>3</sub>	11.00 (0.61)	18.71 (0.45)	19.59 (0.75)	26.19 (2.68)
FeO <sup>b</sup>	17.98 (0.73)	0.25 (0.40)	0.10 (0.08)	0.09 (0.09)
MnO	0.40 (0.12)	0.04 (0.07)	0.04 (0.07)	0.05 (0.08)
MgO	9.79 (0.55)	0.08 (0.20)	0.02 (0.02)	0.27 (1.55)
CaO	11.34 (0.32)	0.04 (0.07)	0.37 (0.25)	7.21 (0.61)
Na <sub>2</sub> O	1.31 (0.14)	0.39 (0.45)	11.22 (1.02)	7.76 (0.71)
K <sub>2</sub> O	1.05 (0.13)	15.14 (1.20)	0.26 (0.46)	0.16 (0.09)
Total	96.72	96.59	99.51	100.03
	Mean	Mean	Mean	Mean
Zn	180 (16)	20 (5)	14 (7)	17 (6)
Pb	73 (26)	23 (4)	19 (4)	27 (17)
Cd	6 (1)	4 (3)	3 (2)	2 (2)
Structural formulae (atoms) <sup>c</sup>				
Si	6.75 (0.07)	3.09 (0.03)	3.17 (0.03)	2.78 (0.04)
<sup>IV</sup> Al	1.25 (0.07)	0.91 (0.03)	0.91 (0.03)	1.22 (0.04)
<sup>VI</sup> Al	0.50 (0.10)	0.03 (0.03)	0.08 (0.04)	0.03 (0.04)
Ti	0.21 (0.06)	0.00 (0.00)	0.00 (0.00)	0.00 (0.01)
Fe <sup>2+</sup>	2.86 (0.13)	0.01 (0.02)	0.00 (0.00)	0.00 (0.00)
Mn	0.06 (0.02)	0.00 (0.00)	0.00 (0.00)	0.00 (0.00)
Mg	1.55 (0.08)	0.00 (0.01)	0.00 (0.00)	0.01 (0.08)
Ca	1.80 (0.05)	0.00 (0.01)	0.02 (0.01)	0.40 (0.03)
Na	0.21 (0.02)	0.02 (0.02)	0.88 (0.04)	0.37 (0.04)
K	0.17 (0.02)	0.94 (0.02)	0.01 (0.02)	0.15 (0.02)

<sup>a</sup>Values in brackets are the standard errors; <sup>b</sup>Total iron expressed as FeO; <sup>c</sup>Formulae calculated on 8 oxygens basis, except amphiboles calculated on 23 oxygens.

from rock-fluid interactions:

$$X_n = [F_v - (da_x/da_y)C_x] - C_y \quad (1)$$

where  $X_n$  is the amount (g) of the oxide n gained ( $X_n > 0$ ) or lost ( $X_n < 0$ ) per 100 grams of rock,  $F_v$  is the volume factor,  $da_x$  and  $da_y$ ,  $C_x$  and  $C_y$  are the apparent densities and the concentrations of the oxide n (wt.%) in the reference and altered rocks respectively. Geochemical mass balances are calculated using either rock volume or concentration of a given element as invariant. Rock alteration usually operates with increasing volume and mass balances are thus currently calculated using Al<sub>2</sub>O<sub>3</sub> or TiO<sub>2</sub> as invariant. In this case, a volume factor ( $F_{vc}$ ) required for a given oxide n to be constant during alteration can be calculated setting  $X_n = 0$  in Equation (1). The  $F_{vc}$

values calculated with TiO<sub>2</sub> as invariant remain very close to unity throughout the two soils (**Figure 2(a)**) and indicate that TiO<sub>2</sub> could be used as the invariant reference for the mass transfer calculation. The CS8 sample, with low loss on ignition and high apparent density (**Table 1**) has suffered very low weathering and was selected as the reference rock. The first chemical change observed in the weathering chemical balances (**Figures 2(b)** and **(c)**) is the general increase in LOI from bottom to top of the two soil profiles (3.77 to 8.53 wt.%). After organic matter destruction and in the absence of carbon dioxide (no carbonate was detected), increasing LOI reflects a general increase in hydrate content with increasing weathering and, more precisely, with increasing hydrated clay minerals and oxyhydroxides formation. Alternatively,

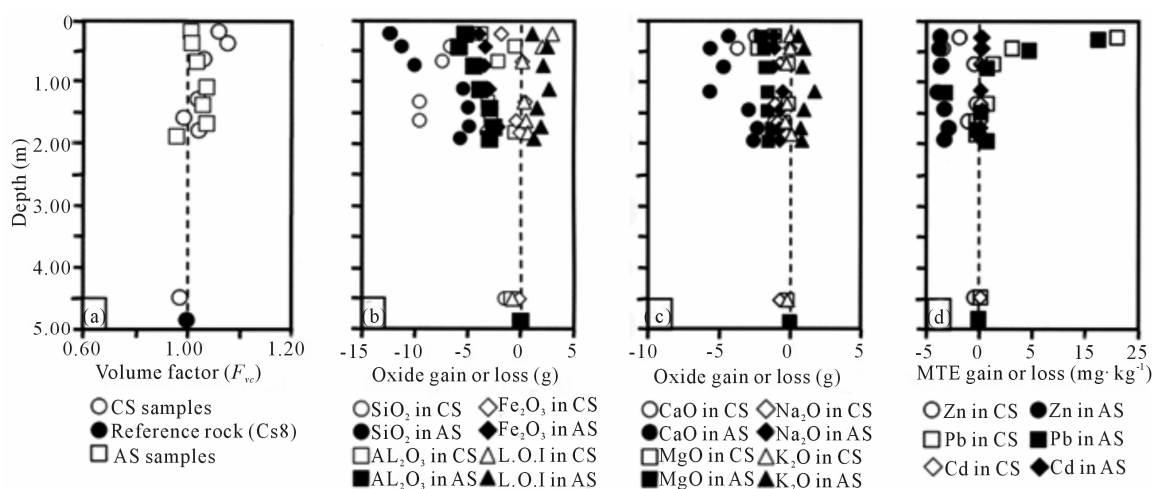


**Figure 2.** Bulk weathering mass balances calculated in amended and control soils using  $\text{TiO}_2$  as invariant: (a) Variations of volume factor; (b) and (c) Mass balances for major elements (LOI: Loss on Ignition); (d) Mass balance for Zn, Pb, and Cd.

all major primary mineral components, except potassium, are continuously leached from rock to soil in variable amounts. The highest leaching rate is given by the  $\text{SiO}_2$  compound, up to 12%,  $\text{Al}_2\text{O}_3$ ,  $\text{Fe}_2\text{O}_3$ , and  $\text{CaO}$  have medium leaching rates about 5% whereas  $\text{MgO}$  and  $\text{Na}_2\text{O}$  display the lowest rates, about 1%. The leaching of  $\text{SiO}_2$ ,  $\text{Al}_2\text{O}_3$ ,  $\text{CaO}$  and  $\text{Na}_2\text{O}$  results for a large part from the dissolution of plagioclases whereas moderate  $\text{MgO}$  leaching points to low amphibole alteration. The constant to low increasing  $\text{K}_2\text{O}$  concentration in saprolite and soil can be attributed to unweathered orthoclase remnants.

Although spread sludges were heavily loaded with Zn, Pb and Cd (498, 330 and 20  $\text{mg}\cdot\text{kg}^{-1}$  as mean concentrations respectively), the MTE vertical profiles obtained from the mass balances (**Figure 2(d)**) do not show Zn and Cd anthropic contamination of the amended soil when compared to the control soil. The bulk Zn concentrations show large variations in the two soils (**Table 1**), from 82 to 126  $\text{mg}\cdot\text{kg}^{-1}$ . The calculated mass balance indicates low Zn depletion in the upper surface horizons of the two soils that may suggest migration of this metal in depth, as already observed [24]. The bulk Cd concentrations given in **Table 2** are under the detection limit in the control soil and range from 0.13 to 0.33  $\text{mg}\cdot\text{kg}^{-1}$  in the amended soil, well below the contamination threshold of 2  $\text{mg}\cdot\text{kg}^{-1}$  [2]. The mass balance calculated for Cd in the amended soil does not show any apparent depletion or accumulation which could induce local contaminations at the scale of the soil or saprolite horizons. The behavior of Pb strongly differs from Zinc and Cd: the bulk Pb concentrations are similar in the two soils (**Table 1**), more than ten times lower than in spread sludges, but increase in both upper horizons CS1 and AS1 samples at 38 and 39  $\text{mg}\cdot\text{kg}^{-1}$ . This behavior is better evidenced in the vertical mass balance profiles where Pb accumulates in the first surface horizons at similar concentrations in

the two soils (**Figure 2(d)**). These similar surface accumulation rates in the two soils suggest that Pb concentrations are not modified by sludge spreading and that surface accumulation could result from atmospheric fallout, as already described [25].

### 3.3. Soil Clay Mineralogy and Chemistry

The  $<2\ \mu\text{m}$  clay fractions extracted from the bulk soil samples have similar mineralogy in the control and amended soils. The smectite is the dominant clay mineral (about 80% of the clayey fraction) with XRD (001) reflections at 15.10 Å in air-dried state shifting to 17.05 Å in ethylene-glycol solvated state. Kaolinite is observed in smaller quantity (about 20% of the clayey fraction) with (001) and (002) reflections at 7.15 Å and 3.55 Å in air-dried state that disappear after 450°C heating.

The EPMA of the MTE in the clay fractions from the two soils (**Table 3**) are plotted versus depth in **Figure 3**. The first observation is that the clay minerals from the amended soil are contaminated with Zn and Cd when compared to the control soil. The Zn contents in the amended soil range from 144 to 203  $\text{mg}\cdot\text{kg}^{-1}$  and are always higher than in control soil (10 to 24  $\text{mg}\cdot\text{kg}^{-1}$ ). The Zn distribution with depth is typically that of a downward migrating element. The highest Zn contents are measured in the upper horizons of the amended soil (AS2 and AS1 samples with 203 and 195  $\text{mg}\cdot\text{kg}^{-1}$  at 0.40 m and 0.20 m depths, respectively). These concentrations decrease progressively to 150  $\text{mg}\cdot\text{kg}^{-1}$  at 1.90 m depth (AS7 sample) whereas Zn contents at this depth in the control soil is almost ten times lower with 14  $\text{mg}\cdot\text{kg}^{-1}$  at 1.80 m depth. The Cd distribution is similar to that of Zn but with much lower values, 17 to 25  $\text{mg}\cdot\text{kg}^{-1}$  in amended soil samples versus 5 to 9  $\text{mg}\cdot\text{kg}^{-1}$  in control soil samples. Alternatively, Pb concentrations measured in the amended and control soils do not show any sig-

**Table 3. EPMA of MTE (Zn, Pb, Cd, mg.kg<sup>-1</sup>) in the bulk clay fractions of control soil (CS) and amended soil (AS) samples.**

Depth	CS8	CS7	CS6	CS5	CS4	CS3	CS2	CS1	AS7	AS6	AS5	AS4	AS3	AS2	AS1
(m)	4.85	4.50	1.80	1.60	1.30	0.65	0.40	0.20	1.90	1.70	1.40	1.10	0.70	0.40	0.20
Zn <sup>a</sup>	15 (1.6)	14 (1.3)	14 (1.8)	17 (2.4)	18 (2.9)	19 (3.2)	24 (4.5)	10 (3.2)	150 (12.3)	158 (11.9)	144 (10.5)	153 (9.8)	177 (8.6)	203 (12.6)	195 (11.8)
Pb	6 (2.5)	7 (2.5)	5 (2.4)	8 (2.3)	9 (4.4)	5 (3.4)	6 (2.8)	4 (1.8)	5 (2.4)	9 (2.1)	11 (1.8)	5 (1.5)	7 (1.6)	10 (1.8)	8 (2.1)
Cd	7 (0.3)	4 (0.2)	5 (0.9)	8 (0.6)	9 (0.5)	7 (0.5)	6 (0.4)	5 (0.8)	17 (1.9)	19 (1.8)	20 (2.1)	24 (1.8)	16 (2.2)	22 (2.1)	25 (1.8)

<sup>a</sup>Each analysis is the result of 10 measurements on the same crystal, values in brackets are the standard errors.

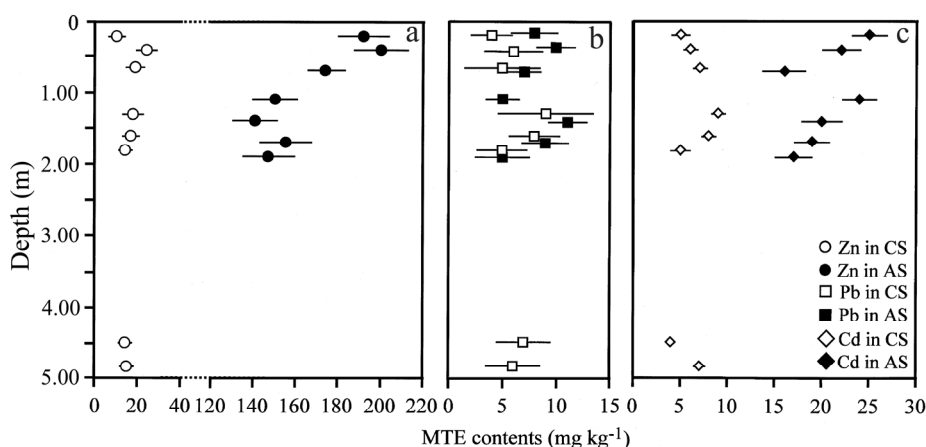


**Figure 3. Vertical distribution profiles of (a) Zn, (b) Pb and (c) Cd concentrations in the clay fractions from the amended soil (AS) and the control soil (CS); error bars are showing the standard errors.**

nificant evolution in the profiles when standard errors are considered.

### 3.4. MTE in Amphiboles

Representative MTE contents in the amphiboles and their weathering clay minerals are given in **Tables 2** and **4**. All data are distributed according to the depth in **Figures 4(a)-(c)**. Early amphibole weathering produces magnesian smectite of saponite-type (sample CS7 in **Table 4**) and leads to the leaching of Zn from 180 mg.kg<sup>-1</sup> in unaltered amphibole to 85 mg.kg<sup>-1</sup> in the magnesian smectite. Such a leaching does not operate for Pb whose concentrations are very closed in amphiboles and clay (73 and 71 mg.kg<sup>-1</sup>), nor for Cd whose contents are close to the detection limits (6 mg.kg<sup>-1</sup> and 3 mg.kg<sup>-1</sup>).

More intense amphibole weathering stages in C, Bw and A soil horizons produce aluminium smectite of montmorillonite-type and result in very different MTE distribution as the control soil or the amended soil is considered (**Figures 4(a)-(c)**). Zn, Pb and Cd contents in the control soil do not exhibit important variations from the bottom to the top of the profile.

More complicated is the MTE distribution in the amended soil. First of all, the concentrations do not change in the levels where amphibole weathers into

saponite, from 4.50 m to 1.70 m depths and, in the second place, concentrations increase in the horizons where amphibole weathers into montmorillonite, from 1.40 m depth to the top of the amended soil. Zn increases from 81 mg.kg<sup>-1</sup> to 220 mg.kg<sup>-1</sup>, Pb from 70 mg.kg<sup>-1</sup> to 125 mg.kg<sup>-1</sup> and Cd from 9 mg.kg<sup>-1</sup> to 42 mg.kg<sup>-1</sup>.

### 3.5. MTE in Plagioclases

Some typical MTE contents in the plagioclases and in their weathering products are listed in **Tables 2** and **4** and the whole set of data is correlated with depth in **Figures 4(d)-(f)**. The first weathering stage of plagioclases at the bottom the control soil produces aluminium smectite of montmorillonite-type (sample CS7 in **Table 4**). This weathering process operates through an increase in Zn and Pb contents from plagioclases to montmorillonites (**Figures 4(d)-(e)**). Zn concentrations increase from 17 mg.kg<sup>-1</sup> in the plagioclase crystal to 66 - 78 mg.kg<sup>-1</sup> in its specific montmorillonite clay mineral, whereas Pb increases from 27 mg.kg<sup>-1</sup> in the plagioclase to 48 - 43 mg.kg<sup>-1</sup> in the montmorillonite. The Cd contents in plagioclases and montmorillonites remain very close without any significant variations (from 2 mg.kg<sup>-1</sup> to 3 - 4 mg.kg<sup>-1</sup>). The weathering of plagioclases in the soil horizons leads to the crystallization of three clay mineral

**Table 4. Representative EPMA of heavy metals (Zn, Pb, Cd, mg·kg<sup>-1</sup>) in clays as weathering products of rock-forming mineral from control soil (CS) and amended soil (AS) samples.**

Depth	Clay minerals in amphiboles						Clay minerals in plagioclases					
	CS7	CS4	CS1	AS7	AS4	AS1	CS7	CS4	CS1	AS7	AS4	AS1
(m)	4.50	1.30	0.20	1.90	1.10	0.20	4.50	1.30	0.20	1.90	1.10	0.20
Zn <sup>a</sup>	85 (7.25)	77 (4.20)	75 (4.40)	72 (7.60)	105 (4.05)	220 (6.20)	66 (10.20)	37 (4.20)	27 (2.40)	67 (7.60)	36 (4.05)	30 (2.10)
Pb	71 (4.75)	75 (6.50)	76 (5.15)	62 (4.60)	94 (3.50)	125 (8.70)	43 (4.75)	41 (3.85)	40 (2.10)	45 (4.60)	39 (3.50)	38 (2.00)
Cd	3 (0.55)	3 (0.60)	3 (0.50)	3 (0.40)	14 (1.20)	42 (2.05)	4 (0.60)	3 (0.90)	2 (0.50)	24 (1.35)	15 (1.20)	12 (2.00)

<sup>a</sup>each analysis is the result of 10 measurements on the same crystal, values in brackets are the standard errors.

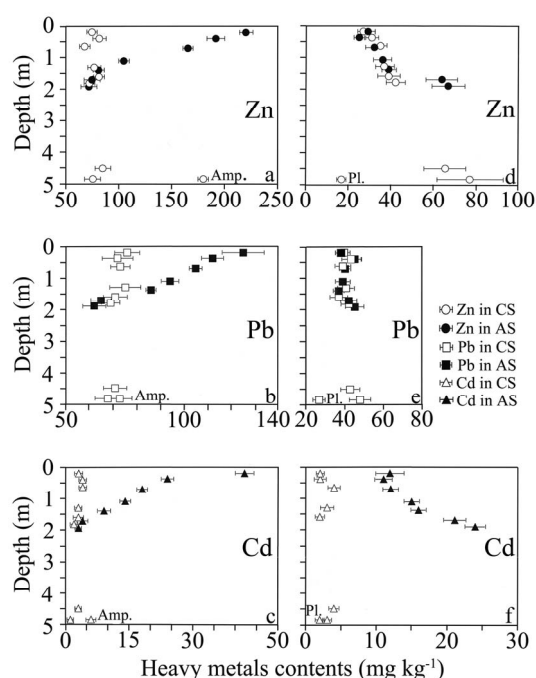


**Figure 4. Distribution of the MTE Zn, Pb, and Cd in the control (open symbols) and amended soil (black symbols) as a function of the amphibole and plagioclase weathering sequences; (a), (b), (c): Zn, Pb, and Cd distributions during the weathering of amphibole (Amp.); (d), (e), (f): Zn, Pb, and Cd distributions during the weathering of plagioclase (Pl.); error bars are showing the standard errors.**

species with well-defined formation horizons. Montmorillonite, already observed at the bottom of the control soil, is present in the C horizon, (1.90 m to 1.40 m depth). The Bw horizon is typified by two random kaolinite/smectite mixed layers (KS) with different kaolinite and smectite components contents. The first K/S with 65% smectite component is found at the bottom of the Bw horizon (1.40 m depth) and the second with only 5% smectite component is found at the top of the Bw horizon (0.70 m depth). The A horizon (from 0.40 m depth to surface) is characterized by the crystallization of kaolinite.

The behaviour of the MTE analysed in the plagioclase weathering products from C, Bw and A horizons depends on 1) the chemical species considered, 2) the type of soil studied (control or amended soil) and 3) the clay mineral species formed in the studied horizon. The Zn contents in the control soil horizons decrease regularly from 42 mg·kg<sup>-1</sup> in the C horizon (1.80 m depth) to 27 mg·kg<sup>-1</sup> in the A horizon at the soil surface (**Figure 4(d)**). Same Zn evolution appears in the amended soil, but with higher contents in the C horizon (67 mg·kg<sup>-1</sup>) when compared to the control soil. This general Zn decrease from bottom to top follows the decrease in smectite contents in the plagioclase weathering products from C, Bw and A horizons (smectite-K/S—kaolinite weathering sequence). The Pb concentrations in the plagioclase weathering products from control soil and amended soil (**Figure 4(e)**) remain very close (42 to 37 mg·kg<sup>-1</sup> in the control soil and 38 to 45 mg·kg<sup>-1</sup> in the amended soil). The small differences in concentrations fall in the range of the standard error (2.00 - 5.30 mg·kg<sup>-1</sup>) and no significant Pb evolution from bottom to top of the soil is observed. The Cd concentrations in the plagioclase weathering products are very different in the two soils (**Figure 4(f)**). The Cd concentrations in the control soil are very low (2.00 to 5.00 mg·kg<sup>-1</sup>) and close to the limits of quantification. No significant variation is observed from bottom to top.

The amended soil shows higher Cd concentrations in the clay minerals derived from the plagioclases (11 to 24 mg·kg<sup>-1</sup>) with a regular decrease from bottom (24 mg·kg<sup>-1</sup>) to top (12 mg·kg<sup>-1</sup>). This Cd decrease is similar to Zn behaviour and follows the same mineralogical trend, *i.e.* the decrease in smectite contents from the C horizon to the A horizon.

#### 4. Discussion

The MTE concentrations in the bulk soil samples (**Table 1**) are always below the baseline values taken as the higher limits for non-contaminated soils in the new French regulations (NF French Standard U 44-041 modi-

fied by Ordinance 97-1133): Zinc concentrations are from 82.00 to 126.08 mg·kg<sup>-1</sup> with 300 mg·kg<sup>-1</sup> baseline, Pb values are from 14.84 to 39.08 mg·kg<sup>-1</sup> with 100 mg·kg<sup>-1</sup> baseline, and Cd ranges from values below analytical detection limit to 0.33 mg·kg<sup>-1</sup> with 2.00 mg·kg<sup>-1</sup> baseline. These results and the calculated mass balances demonstrate that sludge spreadings on the area did not induce Zn, Pb or Cd contamination. These data, however, were collected at the scale of the soil sample and a thorough study of soil components indicates that local Zn, Pb, and Cd concentrations may occur in specific soil particle-size fractions, such as <2 µm clay fraction and weathering microsites at rock-forming mineral scale.

The comparison of the MTE contents in the <2 µm clay fractions in the two soils (**Table 3** and **Figure 3**) reveals clearly anthropic Zn and Cd contaminations of the clay minerals in the amended soil surface horizons (0.20 to 0.40 m depth). This surface contamination is associated with downward migration of Zn and Cd down to 1.90 m depth within the amended soil. Lead concentrations are slightly higher in amended soil without clear evidence for downward migration. Since bulk clay fractions are the collection of the clay minerals formed during the weathering of primary rock-forming minerals, the study of these MTE concentrations is greatly improved by considering clay minerals in their formation sites, *i.e.* the weathering microsites.

The MTE concentration profiles collected from the amphiboles weathering microsites (**Figure 4**) point out a general anthropic contamination of the clay minerals with Zn, Pb, and Cd within the amended soil surface horizons. This surface contamination can be attributed to the clay mineral montmorillonite which appears in large amount from the amphiboles weathering and has a high sorption capacity of 90 to 127 cmol·kg<sup>-1</sup> [26,27]. This surface accumulation is followed in the deeper horizons by a regular decrease in MTE contents, in relation with the decrease in amphibole weathering intensity which produces a decrease in the smectite content, and, as a consequence, a decrease in sorption capacity with depth. Conversely, the MTE concentration profiles obtained from the plagioclases weathering microsites (**Figure 4**) show a Zn and Cd depletion of the clay minerals within the amended soil surface horizons, whereas Pb concentrations do not show any significant evolution from the top to the bottom of the soils. This Zn and Cd surface depletion appears to be controlled by the clay mineral weathering sequence of plagioclases: montmorillonite with high sorption capacity (see above) at the bottom and kaolinite with low sorption capacity of 16 - 34 cmol·kg<sup>-1</sup> [28,29] at the top of the soil profiles. As a consequence, Zn and Cd are not sorbed in the surface horizon and can migrate slowly downwards to more smectitic assemblages (K/S) and finally to montmorillonite where they

are retained (1.90 m depth).

## 5. Conclusions

The results presented in this paper demonstrate that clay minerals are, together with oxides and organic matter, important soil components which play a major role in the mobility of MTE in contaminated soils.

Clays study is essential to understand the sorption reactions occurring at the solid/solution interface in soils. Soils are complex assemblages of clay minerals which formed in weathering microsystems and have a wide range of specific sorption properties. Therefore, there is a need for accurate studies at the scale of these weathering microsystems to identify each clay mineral species and thus to estimate the sorption capacity of the weathering microsite.

This work demonstrates that the micrometric mineralogical approach is relevant to describe the importance of the clay minerals species in the MTE fixation in soil. This mineralogical approach could be of a great interest to improve the modeling of the MTE surface complexation in soils [30].

## REFERENCES

- [1] G. Amon, O. Aznar and D. Vollet, "Why Are Some French Farmers Sludge-Takers? Some Agronomic and Socio-economic Explanations," *International Journal of Agricultural Resources, Governance and Ecology*, Vol. 5, No. 2-3, 2006, pp. 289-308.
- [2] D. Baize, "Teneurs Totales en Eléments Traces Métalliques dans les sols (France)," INRA Editions, Paris, 1997.
- [3] F. M. G. Tack, M. G. Verloo, L. Vanmechelen and E. Van Ranst, "Baseline Concentration Levels of Trace Elements as a Function of Clay and Organic Carbon Contents in Soils in Flanders (Belgium)," *The Science of the Total Environment*, Vol. 201, No. 2, 1997, pp. 113-123. [http://dx.doi.org/10.1016/S0048-9697\(97\)00096-X](http://dx.doi.org/10.1016/S0048-9697(97)00096-X)
- [4] P. Planquart, G. Bonin, A. Prone and C. Massiani, "Distribution, Movement and Plant Availability of Trace Metals in Soils Amended with Sewage Sludge Compost: Application to Low Metal Loadings," *The Science of the Total Environment*, Vol. 241, No. 1-3, 1999, pp. 161-179. [http://dx.doi.org/10.1016/S0048-9697\(99\)00338-1](http://dx.doi.org/10.1016/S0048-9697(99)00338-1)
- [5] R. A. Klassen, "Geological Factors Affecting the Distribution of Trace Metals in Glacial Sediments of Central Newfoundland," *Environmental Geology*, Vol. 33, No. 2-3, 1998, pp. 154-169. <http://dx.doi.org/10.1007/s002540050235>
- [6] D. Baize and T. Sterckeman, "Of the Necessity of Knowledge of the Natural Pedo-Geochemical Background Content in the Evaluation of the Contamination of Soils by Trace Elements," *The Science of the Total Environment*, Vol. 264, No. 1-2, 2001, pp. 127-139. [http://dx.doi.org/10.1016/S0048-9697\(00\)00615-X](http://dx.doi.org/10.1016/S0048-9697(00)00615-X)
- [7] T. Sterckeman, F. Douay, D. Baize, H. Fourier, N. Proix



- and C. Schwartz, "Trace Elements in Soils Developed in Sedimentary Materials from Northern France," *Geoderma*, Vol. 136, No. 3-4, 2006, pp. 912-929. <http://dx.doi.org/10.1016/j.geoderma.2006.06.010>
- [8] I. Walter and G. Cuevas, "Chemical Fractionation of Heavy Metals in a Soil Amended with Repeated Sewage Sludge Application," *The Science of the Total Environment*, Vol. 226, No. 2-3, 1999, pp. 113-119. [http://dx.doi.org/10.1016/S0048-9697\(98\)00374-X](http://dx.doi.org/10.1016/S0048-9697(98)00374-X)
- [9] M. O. Mbila, M. L. Thompson, J. S. C. Mbagwu and D. A. Laird, "Distribution and Movement of Sludge-Derived Trace Metals in Selected Nigerian Soils," *Journal of Environmental Quality*, Vol. 30, No. 5, 2001, pp. 1667-1674. <http://dx.doi.org/10.2134/jeq2001.3051667x>
- [10] E. Steinnes, R. O. Allen, H. M. Petersen, J. P. Rambaek and P. Varskog, "Evidence of Large Scale Heavy-Metal Contamination of Natural Surface Soils in Norway from Long-Range Atmospheric Transport," *The Science of the Total Environment*, Vol. 205, No. 2-3, 1997, pp. 255-266. [http://dx.doi.org/10.1016/S0048-9697\(97\)00209-X](http://dx.doi.org/10.1016/S0048-9697(97)00209-X)
- [11] L. Hernandez, A. Probst, J. L. Probst and E. Ulrich, "Heavy Metal Distribution in Some French Forest Soils: Evidence for Atmospheric Contamination," *The Science of the Total Environment*, Vol. 312, No. 1-3, 2003, pp. 195-219. [http://dx.doi.org/10.1016/S0048-9697\(03\)00223-7](http://dx.doi.org/10.1016/S0048-9697(03)00223-7)
- [12] O. Sukreeyapongse, P. E. Holm, B. W. Strobel, S. Panichsakpatana, J. Magid and H. C. B. Hansen, "PH-Dependent Release of Cadmium, Copper, and Lead from Natural and Sludge-Amended Soils," *Journal of Environmental Quality*, Vol. 31, No. 6, 2002, pp. 1901-1909. <http://dx.doi.org/10.2134/jeq2002.1901>
- [13] J. Bang and D. Hesterberg, "Dissolution of Trace Element Contaminants from Two Coastal Plain Soils as Affected by pH," *Journal of Environmental Quality*, Vol. 33, No. 3, 2004, pp. 891-901. <http://dx.doi.org/10.2134/jeq2004.0891>
- [14] M. C. Chuan, G. Y. Shu and J. C. Liu, "Solubility of Heavy Metals in a Contaminated Soil: Effects of Redox Potential and pH," *Water, Air, and Soil Pollution*, Vol. 90, No. 3-4, 1996, pp. 543-556. <http://dx.doi.org/10.1007/BF00282668>
- [15] M. J. Wilson, "Weathering of the Primary Rock-Forming Minerals: Processes, Products and Rates," *Clay Minerals*, Vol. 39, No. 3, 2004, pp. 233-266. <http://dx.doi.org/10.1180/0009855043930133>
- [16] J. Caillaud, D. Proust and D. Righi, "Weathering Sequences of Rock-Forming Minerals in a Serpentinite: Influence of Microsystems on Clay Mineralogy," *Clays and Clay Minerals*, Vol. 54, No. 1, 2006, pp. 87-100. <http://dx.doi.org/10.1346/CCMN.2006.0540111>
- [17] D. Proust, J. Caillaud and C. Fontaine, "Clay Minerals in Early Amphibole Weathering: Tri- to Dioctahedral Sequence as a Function of Crystallization Sites in the Amphibole," *Clays and Clay Minerals*, Vol. 54, No. 3, 2006, pp. 351-362. <http://dx.doi.org/10.1346/CCMN.2006.0540306>
- [18] K. S. Camuti and P. T. McGuire, "Preparation of Polished thin Sections from Poorly Consolidated Regolith and Sediment Material," *Sedimentary Geology*, Vol. 128, No. 1-2, 1999, pp. 171-178. [http://dx.doi.org/10.1016/S0037-0738\(99\)00073-1](http://dx.doi.org/10.1016/S0037-0738(99)00073-1)
- [19] M. Fialin, H. Rémy, C. Richard and C. Wagner, "Trace Element Analysis with the Electron Microprobe: New Data and Perspectives," *American Mineralogist*, Vol. 84, No. 1-2, 1999, pp. 70-77.
- [20] R. L. Gresens, "Composition-Volume Relationships of Metasomatism," *Chemical Geology*, Vol. 2, No. 1, 1967, pp. 47-65. [http://dx.doi.org/10.1016/0009-2541\(67\)90004-6](http://dx.doi.org/10.1016/0009-2541(67)90004-6)
- [21] D. L. Biddle, D. J. Chittleborough and R. W. Fitzpatrick, "An Algorithm to Model Mass Balances Quantitatively," *Computers and Geosciences*, Vol. 24, No. 1, 1998, pp. 77-82. [http://dx.doi.org/10.1016/S0098-3004\(97\)00125-8](http://dx.doi.org/10.1016/S0098-3004(97)00125-8)
- [22] P. Baveye, M. B. McBride, D. Bouldin, T. D. Hinesly, M. S. A. Dahdoh and M. F. Abdel-sabour, "Mass Balance and Distribution of Sludge-Borne Trace Elements in a Silt Loam Soil Following Long-Term Applications of Sewage Sludge," *The Science of the Total Environment*, Vol. 227, No. 1, 1999, pp. 13-28. [http://dx.doi.org/10.1016/S0048-9697\(98\)00396-9](http://dx.doi.org/10.1016/S0048-9697(98)00396-9)
- [23] B. Minasny, A. B. McBratney and S. Salvador-Blanes, "Quantitative Models for Pedogenesis—A Review," *Geoderma*, Vol. 144, No. 1-2, 2008, pp. 140-157. <http://dx.doi.org/10.1016/j.geoderma.2007.12.013>
- [24] P. O. Skokart, K. Meeus-Verdinne and R. De Borger, "Mobility of Heavy Metals in Polluted Soils near Zinc Smelters," *Water, Air, and Soil Pollution*, Vol. 20, No. 4, 1983, pp. 451-463. <http://dx.doi.org/10.1007/BF00208519>
- [25] G. Merrington and B. J. Alloway, "The Flux of Cd, Cu, Pb and Zn in Mining Polluted Soils," *Water, Air, and Soil Pollution*, Vol. 73, No. 1, 1994, pp. 333-344. <http://dx.doi.org/10.1007/BF00477997>
- [26] F. Ayari, E. Srasra and M. Trabelsi-Ayadi, "Characterization of Bentonitic Clays and Their Use as Adsorbent," *Desalination*, Vol. 185, No. 1-3, 2005, pp. 391-397. <http://dx.doi.org/10.1016/j.desal.2005.04.046>
- [27] J. Srodon and D. K. McCarty, "Surface Area and Layer Charge of Smectite from CEC and EGME/H<sub>2</sub>O-Retention Measurements," *Clays and Clay Minerals*, Vol. 56, No. 2, 2008, pp. 155-174. <http://dx.doi.org/10.1346/CCMN.2008.0560203>
- [28] A. P. Ferris and W. B. Jepson, "The Exchange Capacities of Kaolinite and the Preparation of Homoionic Clays," *Journal of Colloid and Interface Science*, Vol. 51, No. 2, 1975, pp. 245-259. [http://dx.doi.org/10.1016/0021-9797\(75\)90110-1](http://dx.doi.org/10.1016/0021-9797(75)90110-1)
- [29] C. Ma and R. A. Eggleton, "Cation Exchange Capacity of Kaolinite," *Clays and Clay Minerals*, Vol. 47, No. 2, 1999, pp. 174-180. <http://dx.doi.org/10.1346/CCMN.1999.0470207>
- [30] J. Hizal and R. Apak, "Modeling of Copper (II) and Lead (II) Adsorption on Kaolinite-Based Clay Minerals Individually and in the Presence of Humic Acid," *Journal of Colloid and Interface Science*, Vol. 295, No. 1, 2006, pp. 1-13. <http://dx.doi.org/10.1016/j.jcis.2005.08.005>